Jornadas de Automática

Industrial Flash Dryer Model Calibration and Validation Using Historical Data

Saeed Rasekhi[a,*], Rogelio Mazaeda[a], Fernando Tadeo[a], Carlos Gomez Palacín[b], Ángel García Bombin[b]

[a] *Department of Systems and Automation, University of Valladolid, School of Industrial Engineering, Pso. Prado de la Magdalena 3-5, 47011 Valladolid, España.*
[b] *SONAE ARAUCO, Calle Títulos, 29, 47009 Valladolid, España.*

To cite this article: Rasekhi, S., Mazaeda, R., Tadeo, F., Gomez Palacín, C., García Bombin Á. 2026. Industrial Flash Dryer Model Calibration and Validation Using Historical Data. Jornadas de Automática, 47. https://doi.org/10.17979/ja-cea.2026.47.13857

Resumen

La calibración y validación de modelos dinámicos de primeros principios en plantas industriales son especialmente complejas debido a la limitada calidad y disponibilidad de datos. Este trabajo presenta la calibración y validación de un modelo distribuido de un secador flash industrial y sus equipos asociados utilizando únicamente datos históricos de producción. Para compensar la ausencia de excitación activa del proceso, se implementó una estrategia de selección de datos que identificó periodos operativos con máxima variabilidad natural. El estudio también aborda retos prácticos relevantes en un entorno industrial real, como perturbaciones no medidas, sincronización entre señales rápidas de sensores y mediciones de laboratorio retardadas, e incertidumbre experimental inevitable. El modelo fue calibrado y validado con conjuntos de datos independientes de la fábrica de SONAE en Valladolid. Los resultados demuestran que datos históricos cuidadosamente seleccionados permiten estimar parámetros fundamentales y obtener una herramienta predictiva robusta para optimización industrial.

Palabras clave: Modeling of manufacturing operations, Process optimization, Model calibration, Closed-loop identification, Experiment design.

Industrial Flash Dryer Model Calibration and Validation Using Historical Data

Abstract

Calibrating and validating dynamic first-principles models in industrial plants is challenging due to limited and imperfect data. This work presents the calibration and validation of a distributed-parameter model for an industrial flash dryer and related equipment using only historical production data. To compensate for the lack of active process excitation, a data-selection strategy is used to identify those operating periods with maximum natural variability. The study also highlights key practical challenges encountered in a real factory environment, including unmeasured process disturbances, synchronization of high-frequency sensor data with delayed laboratory measurements, and unavoidable measurement uncertainty. The model was calibrated and validated with independent datasets from the SONAE factory in Valladolid. Results show that, despite data-quality limitations and closed-loop operating conditions, carefully selected historical data can successfully estimate fundamental parameters and provide a reliable predictive tool for industrial optimization.

Keywords: Modeling of manufacturing operations, Process optimization, Model calibration, Closed-loop identification, Experiment design.

*Autor para correspondencia: saeed.rasekhi@uva.es

1. Introduction

Convective pneumatic flash drying of wood fiber is a highly energy-intensive and critical manufacturing stage in Medium-Density Fiberboard (MDF) production. The processing sequence requires drying wet wood fibers produced via pressurized mechanical defibration to strict moisture levels of 10–20% (0.1–0.2 kg of water/kg of dry wood) before resin blending and hot pressing. Achieving accurate dynamic regulation of the outlet fiber moisture is complicated by highly non-linear transport phenomena, strong structural couplings between the thermal and mass fields, and input disturbances such as changing ambient conditions and raw material fluctuations.

To surpass the limitations of conventional black-box representations that fail to resolve intermediate internal states, a high-fidelity distributed grey-box model was developed, coupling a Finite Volume Method (FVM) along the dryer tube (Rasekhi et al., 2025) with a lumped transient representation of the downstream cyclone collector. However, deploying such first-principles models as an active industrial digital twin requires parameter calibration and validation.

The diagram in Figure 1 illustrates a pneumatic wood fiber drying system controlled by a PID controller. Hot combustion gas and ambient air are mixed and regulated through adjustable air flaps before entering the dryer system. Preheated wood fiber and steam are injected into the hot airflow, and a fan moves the mixture through the dryer tube, where moisture is rapidly removed from the fibers. Temperature sensors placed at different points continuously monitor the process and send feedback to the PID controller, which automatically adjusts airflow and temperature to maintain efficient and consistent drying conditions. Finally, the dried fiber is separated and collected at the outlet for further processing.

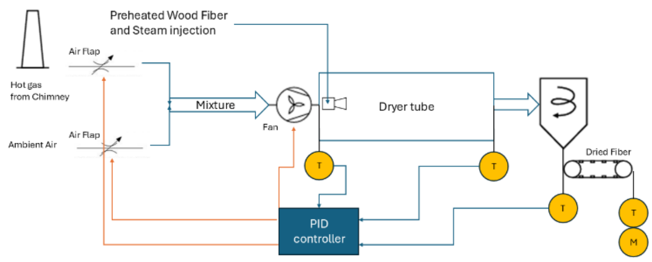

Figure 1: The MDF dryer schematic at SONAE Arauco's facilities.

This paper investigates the fundamental challenges encountered during the physical calibration and validation phases of the digital twin system under real industrial operating conditions. In practice, production plants operate continuously under regulatory automation frameworks, primarily based on closed-loop proportional–integral–derivative (PID) control architectures. Data collected under closed-loop operation inherently introduces systematic cross-correlation between unmeasured stochastic process disturbances and feedback control actions. Consequently, applying direct optimization or classical prediction-error identification methods to such data, without enough excitation performed either in open loop or in closed loop by guaranteeing adequate and frequent changes in the references, leads to biased parameter estimates that obscure the true underlying process physics. Moreover, due to production continuity requirements and plant safety constraints, the implementation of aggressive open-loop excitation signals, such as Pseudo-Random Binary Sequences (PRBS), is often impractical or prohibited. Therefore, this study relies primarily on historical industrial operating data for model calibration and strongly recommends implementing constrained closed-loop well-designed experiments (DOE) within acceptable production limits (Forssell & Ljung, 1999).

To address these limitations, the work presents a programmatic mitigation framework based on global Bayesian optimization routines configured for parameter estimation under closed-loop operational constraints. The study concludes with a comprehensive parameter sensitivity analysis and validation against measurements obtained from the industrial production plant.

2. Mathematical Modeling and Simulation Framework

The dynamic behavior of the convective pneumatic drying process is modeled using a coupled set of multi-phase partial differential equations (PDEs) resolved across two interconnected domains: the 1D axially distributed dryer tube and the lumped-parameter cyclone separator.

2.1. Flash Dryer (FVM Implementation)

The dryer is treated as a one-dimensional cylindrical domain of length (Rasekhi et al., 2025). The system states track five primary variables: fiber temperature (T_f), fiber moisture (H_f), air temperature (T_a), air specific humidity (H_a), and pipe wall temperature (T_p). The domain is spatially discretized into n_d=50 finite volume cells with uniform grid spacing $dx = L/n_d$ for the dryer, although n_c=5 for the cyclone. The mass and energy equations for each cell are governed by the physical property formulas:

$$Sc = \frac{mu_{air}}{\rho_{air} \times diff_{vap\_air}} \tag{1}$$
$$K_c = \frac{h}{\rho_{air} \times Cp_{air}} \times (\frac{Sc}{Pr_{air}})^{\frac{2}{3}}$$

Where ρ (density), diff (molecular diffusion coefficient of water vapor in air), Sc (Schmidt number), Pr (Prandtl number), Cp (Specific heat), and Kc represent the mass transfer coefficient. The subscripts used are: a (air), f (fiber), p (pipe), env (environment), and vap (vapor). While air pushes the wood fiber to flow through the dryer tube, v_f and v_a represent the calculated phase velocities containing slip velocity dynamics derived from standard drag expressions (Perry and Green, 1984). The fundamental multi-phase transport equations and boundary layer film theories governing these interactions follow standard convective transport formulations (Bird et al., 2002; Incropera and DeWitt, 2007). The humid air thermophysical properties and density are updated explicitly using standard thermodynamic formulations (Moran and Shapiro, 2010; ASHRAE, 2017). The drying kinetic rate incorporates a continuous double-sigmoid reduction coefficient $\alpha(H_f)$ to describe the transition from free surface evaporation to bound-water internal diffusion regimes without numerical discontinuities (Pang, 2001):

(2)

$$K_{evap} = K_c \times \rho_{air} \times \frac{Qm_{fiber}}{\rho_{fiber}} \times mult_D$$
$$dM_{dry} = \frac{\alpha(H_f) \times K_{evap} \times A_{vol} \times (H_f - H_a)}{Qm_{fiber}}$$
$$\frac{dT_{fiber}}{dt} = h_{a\_f} \times mult_h + \left(\frac{H_{Wv} \times dM_{dry}}{Cp_f}\right)$$
$$\frac{dT_{air}}{dt} = \frac{h_{a\_p} \times Primeter_{pipe} \times (T_{air} - T_{pipe})}{\rho_{air} \times Cp_{air} \times Area_{air}}$$
$$\frac{dT_{pipe}}{dt} = \frac{mult_p}{R_{pipe}} \times \frac{(T_{pipe} - T_{env})}{\rho_{pipe} \times Cp_{pipe} \times Area_{pipe}}$$
$$\frac{dT_{pipe}}{dt} = \frac{k_p \times mult_k \times Across_p}{dx^2} \times (T_{p_{i-1}} - 2T_{p_i} + T_{p_{i+1}})$$

Where A_{vol} represents the specific fiber contact area per unit volume (m^2/m^3), $\alpha(H_f)$ is a Sigmond function for the water evaporation rate in wood, which represents the transition from free surface evaporation to bound-water internal diffusion, as well as the underlying wood fiber thermophysical properties, modeled based on the comprehensive wood property (Dietenberger, 2002). The subscripts used are: evap (evaporation), vol (volumetric), a_p (air to pipe), a_f (air to fiber), vap (vapor), dry (dryer), and cyc (cyclone). The multiplier parameter $mult_D$ was added to the model to perform the calibration and optimization in the dryer part, as well as $mult_h$ for heat transfer between air and fiber, $mult_k$ for heat conduction through the steel pipe, and $mult_p$ for external heat transfer from the dryer pipe to the environment, which is structurally derived using the classical cylinder crossflow correlations for forced convection proposed by A Correlating Equation (Churchill et al., 1977).

2.2. *Cyclone Domain (Lumped Parameterization)*

At the dryer exit, the multi-phase stream enters a vertical cyclone separator. The classic slip relation is replaced by explicit dynamic particle drag vectors balancing gravity and swirling fluid flows. Because of the lack of measurement data in the cyclone part, we introduced a lumped model, which is a simplified evaporation formula to mimic the behavior of the cyclone separator with respect to the physics of the model.

$$dM_{cyc} = hm_{cyc} \times A_{vol} \times \frac{H_{fiber} - H_{air}}{Qm_f} \qquad (3)$$
$$\frac{dT_{fiber}}{dt} = hc_{cyc} \times A_{vol} \times \frac{(T_{air} - T_{fiber})}{\rho_{fiber} \times Cp_{fiber}}$$

Where hm_{cyc} is the evaporation factor, and hc_{cyc} is the heat transfer coefficient, as well as $mult_C$ (used in Formula 2 instead of $mult_D$ for the evaporation), are optimization parameters in the lumped model in the cyclone. The bounded formulas and the model's physics do not allow us to use any free parameters. The sets of equations (1) to (3) are representations of the mathematical model, yielding modified equations from previous studies (Pang, 2001), (Rasekhi, 2025).

The combined system yields a large, stiff system of ordinary differential equations solved in Python utilizing the Method of Lines (MoL) To isolate accurate physics under these data restrictions, we implemented a gray-box bounding calibration scheme. Instead of treating every individual physical constant as a free variable, the calibration isolates the optimization space to seven global dimensionless scaling multipliers, preserving the mathematical relationships verified by first principles. The designated search domains are detailed in Table 1.

Table 1: Physical Scaling Parameters and Boundaries for Calibration

Parameter	Description	Domain	Optimization Range
$mult_D$	Evaporation rate multiplier	Dryer	[0.01, 5.0]
$mult_C$	Evaporation rate multiplier	Cyclone	[0.01, 5.0]
$mult_h$	Convective heat transfer multiplier	Dryer	[0.01, 5.0]
$mult_k$	Thermal conductivity multiplier	Dryer	[0.01, 5.0]
$mult_p$	External heat loss resistance multiplier	Dryer & Cyclone	[0.01, 5.0]
hm_{cyc}	Evaporation rate coefficient	Cyclone	[1e-7, 0.001]
hc_{cyc}	Heat transfer coefficient	Cyclone	[1.0, 200.0]

3.3. *Algorithmic Formulation (Optimization Engine)*

The calibration task is formulated as a trajectory matching optimization problem executed via Bayesian Optimization using the Tree-structured Parzen Estimator (TPE) sampler in Optuna (Akiba T. et al., 2019), an open-source software. Optuna automates the search process by combining efficient Bayesian optimization samplers with an aggressive imperative pruning mechanism. This dynamically terminates poorly performing trials early in the training phase. This combination significantly reduced our overall computational overhead while successfully discovering a highly robust and optimal hyperparameter configuration. The objective cost function computes a weighted sum of root-mean-square errors (RMSE) between measured historical data outputs and corresponding simulated model states:

$$J = \sum_{m=1}^{M} WF_m \times \sqrt{\frac{1}{N} \times \sum_{k=1}^{N} (y_{real_{m,k}} - y_{model_{m,k}})^2} \qquad (4)$$

Where M is the collection of compared tracking channels, and WF_m represents the specific priority weights factor assigned to balance scale differences between thermal (K) and moisture content (kg/kg) spaces, with respect to their numerical values (temperature weight factors = 0.003, moisture weight factors = 5.0), used both for calculating the residuals and combined sensitivity. To protect validation integrity from initial state contamination, the algorithm uses a "per trial" strategy to compute consistent starting vectors on each execution. Instead of evaluating the parameter space randomly or via costly gradient-based methods that struggle with non-convex mathematical problems, Optuna's TPE algorithm applies Bayes' rule by modeling the parameter probability space using two distinct probability density functions: l(θ) for parameter sets yielding cost values below a specific quantile threshold gamma (successful trials), and g(θ) for remaining combinations (unsuccessful trials). The algorithm iteratively maximizes the Expected Improvement (EI) by sampling candidates from the region where the ratio l(θ) / g(θ) is highest, guiding the dimensionless multipliers toward global convergence (J) while identifying structural sensitivities via functional ANOVA (fANOVA). These configurations were used for optimization: The automated calibration framework was built on top of the open-source Optuna hyperparameter optimization engine using a Tree-structured Parzen Estimator (TPE) Bayesian algorithm. Gamma=0.1, number of trials = 200, PDE solver=BDF, data feeding= resampling 600s, computational runtime = 4.2 hours on an Intel i9 64GB RAM workstation, converging after 82 iterations.

3.4. *Local Parameter Identifiability and Sensitivity*

To formally evaluate the structural identifiability of the gray-box model scaling multipliers ($\theta = [mult_D, mult_C, mult_h, mult_k, mult_p, hm_{cyc}, hc_{cyc}]^T$) under closed-loop data constraints, local parameter sensitivity trajectories were computed. The local sensitivity of a predicted system output state y(t, θ) with respect to a parameter θ is defined by the scaled partial derivative vector:

$$S_i(t) = \theta_i \times \frac{\partial y(t,\theta)}{\partial \theta_i} \tag{5}$$

$$J_{relative} = \frac{\partial y}{\partial \theta_i} \times \frac{\theta_i}{y_{mean}}$$

$$FIM_{combined} = \sum_{m=1}^{M} \frac{1}{\sigma^2} (WF_m)^2 \times (J_m^T J_m)$$

Figure 2 demonstrates dynamic sensitivity trajectories, which represent the absolute change in the output metric per unit of fractional change in the parameter value.

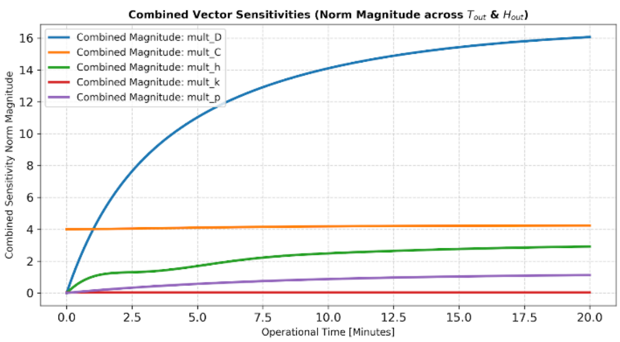

Figure 2: Dynamic sensitivity trajectories with respect to both outlet temperature and moisture.

Another important aspect of the model is to analyze the sensitivity of the model to input variables, most importantly the air temperature, which has a key role in the drying process.

In Figure 3, the sensitivity of the model is demonstrated by the profile of the temperature in the dryer tube. The scale of the temperature data has been removed due to the confidentiality of the data at the SONAE company.

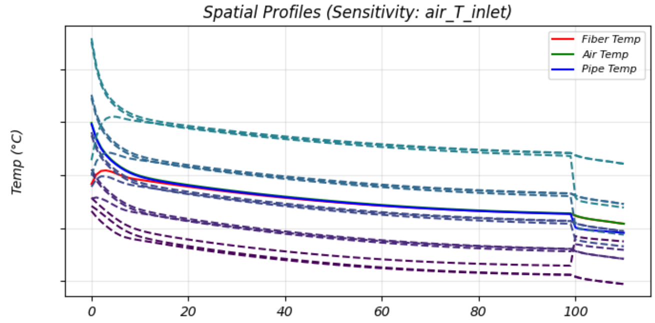

Figure 3: Sensitivity response of the model to changes in inlet air temperature.

The sensitivity analysis on the model parameters helps us determine which parameters have less dependency and correlation with each other, and to choose them for optimization.

3.5. *Calibration Progression Analysis*

Developing and optimizing the model calibration layout required distinct algorithmic execution stages to isolate parameter values under data constraints. To establish structural balance across both mass and energy fields, a balanced cross-variable cost weighting was performed. The comprehensive relative parameter importance analysis computed via fANOVA for this finalized configuration is demonstrated in Figure 4.

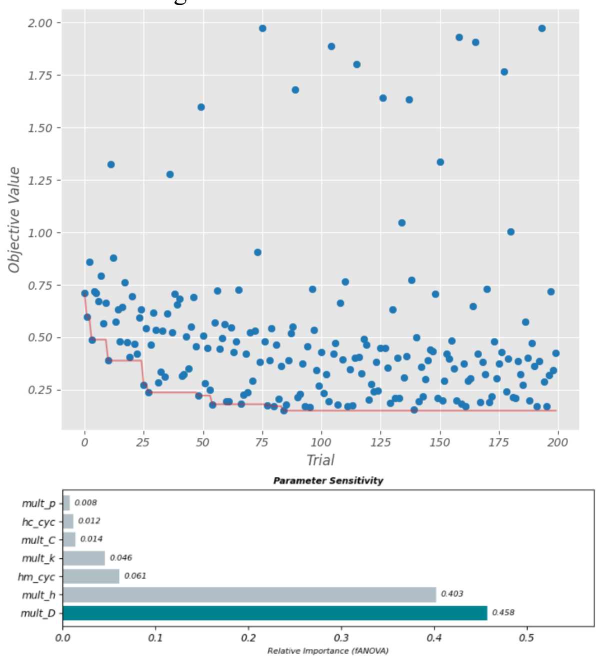

Figure 4: (top) Evolution of the cost function by trial; (bottom) Importance of parameters (fANOVA).

This fANOVA breakdown confirms that the core dryer evaporation scaling factor ($mult_D$) governs nearly 50% of the overall dynamic system sensitivity. Intriguingly, the cyclone evaporation multiplier factor ($mult_C$) registers an importance score of only 0.014.

The calibration results with the best performance optimization are shown in Figure 5, which occurred after 104 iterations. The calibration results in weighted RMSEs of dryer outlet temperature, cyclone outlet temperature, and cyclone outlet moisture are: 0.04 (~13 K), 0.02 (~7 K), and 0.11 (~2.2%).

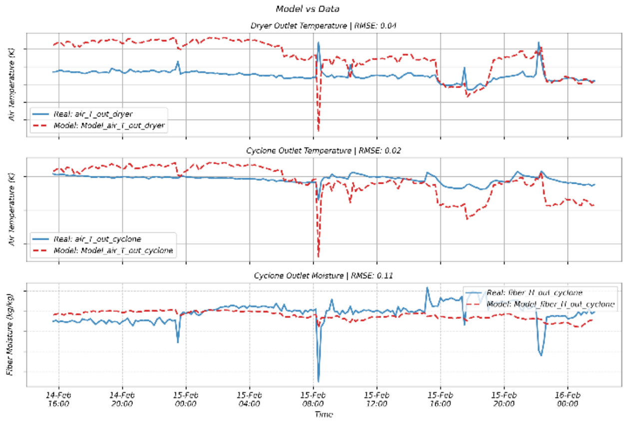

Figure 5: Calibration with the best optimization result. (due to the confidentiality of the data, the numerical axis has been removed)

The best optimized parameters are presented in Table 2. Due to the use of a lumped model, the cyclone evaporation and heat transfer parameters (hm_{cyc}, hc_{cyc}) were optimized directly (not as a multiplier).

Table 2: Optimized parameter values

Parameter	Optimized Value
$mult_D$	0.11815
$mult_C$	0.10064
$mult_h$	0.08552
$mult_k$	4.28099
$mult_p$	3.63673
hm_{cyc}	0.0007
hc_{cyc}	55.667

Table 3 provides the FIM (Fisher Information Matrix) adjusted by their respective priority weighting factors ($WF_{temperature}$=0.003, $WF_{moisture}$=5.0) for the optimized parameters, with a condition number = 5.842e2.

Table 3: Fisher Information Matrix

	$mult_D$	$mult_C$	$mult_h$	$mult_k$	$mult_p$	hm_{cyc}	hc_{cyc}
$mult_D$	4.82e3	-1.10e2	1.43e3	3.15e1	-8.45e1	5.12e2	1.11E1
$mult_C$	-1.10e2	3.55e3	-2.11e2	1.02e1	4.41e1	-1.24e2	-6.80e0
$mult_h$	1.43e3	-2.11e2	5.11e3	5.42e1	-1.12e2	3.95e2	2.43e1
$mult_k$	3.15e1	1.02e1	5.42e1	1.89e2	-2.13e1	1.45e1	1.05e0
$mult_p$	-8.45e1	4.41e1	-1.12e2	-2.13e1	2.44e2	-3.11e1	-2.90e0
hm_{cyc}	5.12e2	-1.24e2	3.95e2	1.45e1	-3.11e1	6.21e4	3.15e2
hc_{cyc}	1.11e1	-6.80e0	2.43e1	1.05e0	-2.90e0	3.15e2	1.08e2

3.6. Validation Results

The predictive accuracy of the calibrated model was evaluated against a raw plant production historical dataset that was excluded from the parameter optimization phase, and the results are presented in Figure 6.

The validation results demonstrate that the calibrated grey-box model successfully captures the core multi-phase transport phenomena and thermal dynamics of the industrial system, successfully following the main trend, while the variations are larger, yielding weighted RMSEs of dryer outlet temperature, cyclone outlet temperature, and cyclone outlet moisture: 0.02 (6.6 K), 0.02 (6.6 K), and 0.12 (2.4%). As illustrated in the validation subplots, the simulated model trajectories track the dynamic trend.

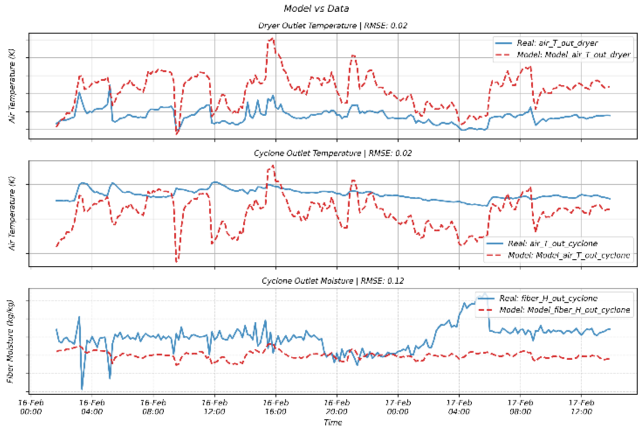

Figure 6: Validation with the best optimization result. (Due to the confidentiality of the data, the numerical axis has been removed)

The validation results demonstrate that the calibrated grey-box model successfully captures the core multi-phase transport phenomena and thermal dynamics of the industrial system, successfully following the main trend while the variations are larger, yielding a remarkably low Root-Mean-Square Error RMSE of 0.02 for both the dryer and cyclone outlet temperatures. As illustrated in the validation subplots, the simulated model trajectories tightly track the dynamic, high-frequency directional swings of the actual plant sensors over a 48-hour production horizon. However, the cyclone outlet moisture validation presents a higher RMSE of 0.12, accurately maintaining the flat, tightly regulated operational baseline but failing to anticipate a sharp moisture surge near the end of the timeline. This specific divergence highlights the impact of unmeasured process disturbances and closed-loop feedback interactions; because inlet fiber moisture is not directly measured and the automated air flappers operate under tight PID regulation, unlogged upstream fluctuations act as an unmodeled hurdle that the current deterministic model parameters cannot fully reconstruct without explicit flappers and raw material dynamics.

This attenuation of variability stems from idealized model assumptions and the impact of severe unmeasured process disturbances. Structurally, the model assumes thermodynamics are dominated by pure wood fibers and water vapor, omitting the rheological effects of chemical additives—such as urea-formaldehyde resins, paraffin wax, and catalysts—which alter the equilibrium moisture content and introduce unmodeled localized reactions. More importantly, the current framework operates under a decoupled inlet boundary condition that cannot account for massive variations originating from the upstream thermomechanical refining process (the defibrator). Continuous fluctuations in raw wood chip species mix, seasonal chip moisture, and mechanical wear on the refiner plates dynamically alter the fiber morphology and specific surface area (A_{vol}), causing rapid, unlogged shifts in physical drying kinetics. Because the inlet fiber moisture (H_f) is not measured directly at the turbulent blowline and the automated mixing air flappers operate under tight regulatory feedback PID loops to stabilize outlet temperatures, these closed-loop actions actively mask the thermal signature of incoming mass-balance variations. Consequently, the unmeasured humidity coming with the fiber acts as an invisible hurdle that a purely deterministic simulation cannot fully reconstruct. This structural limitation underscores the model's true value when embedded as a critical predictive virtual sensor within the factory-wide digital twin ecosystem proposed by (de Prada et al., 2025).

3. Conclusion and Future Work

Validation yielded a cumulative weighted RMSE of 0.17 on a normalized scale, proving that high-variability historical data can successfully calibrate complex first-principles models for industrial digital twins without aggressive open-loop excitation.

Future research identifies four key avenues:

Upstream Mitigation: Integrating wood chip and defibration variations into inlet boundary conditions to prevent unmodeled non-linear behaviors.

Uncertainty Quantification: Investigating a stochastic parameter estimation layer to provide probabilistic confidence intervals.

Air Flapper Modeling: Implementing a dynamic transient model for PID-controlled flappers to decouple fixed-lift operating regime modeling gaps (Santos et al., 2020).

Closed-Loop DOE: Implementing safe, localized closed-loop Design of Experiments using non-intrusive setpoint dither signals to enrich the operational frequency spectrum and resolve severe parameter cross-correlations.

Acknowledgments

This work is part of the Project "Industrial Modernization Promoting Autonomous Control Technologies" (IMPACT) approved by the Ministry of Science in Spain: CPP2024-011491 financiado por MICIU/AEI/10.13039/501100011033/ FEDER, UE; at departamento Ingeniería de Sistemas y Automática, Instituto de Procesos Sostenibles, Escuela de Ingenierías Industriales, Universidad de Valladolid, Spain.

References

Akiba, T., Sano, S., Yanase, T., Ohta, T., Masanori, K., 2019. Optuna: A Next-generation Hyperparameter Optimization Framework. In KDD. Proceedings of the 25th (ACM SIGKDD) International Conference on Knowledge Discovery and Data Mining. DOI: 10.1145/3292500.3330701

ASHRAE, 2017. ASHRAE Handbook - Fundamentals. American Society of Heating, Refrigerating and Air-Conditioning Engineers, Atlanta, GA.

Bird, R. B., Stewart, W. E., Lightfoot, E. N., 2002. Transport Phenomena, 2nd ed. John Wiley & Sons, New York.

Byrne, G. D., Hindmarsh, A. C., 1975. A Polyalgorithm for the Numerical Solution of Ordinary Differential Equations. ACM Transactions on Mathematical Software, 1(1), 71-96. DOI: 10.1145/355626.355636

Churchill, S. W., Bernstein, M., 1977. A Correlating Equation for Forced Convection from Gases and Liquids to a Circular Cylinder in Crossflow. Journal of Heat Transfer, 99(2), 300-306. DOI: 10.1115/1.3450685

de Prada, C., Oliveira da Silva, E., Palacín, C., Vicente, A., García, Á., Tadeo, F., 2025. Gemelo digital para operar planta de producción de tableros MDF. XLVI Jornadas de Automática, 46, 1–8. DOI: 10.17979/ja-cea.2025.46.12176

Dietenberger, M. A., 2002. A Comprehensive Model for the Thermophysical Properties of Wood. Wood and Fiber Science, 34(4), 690-703.

Forssell, U. and Ljung, L. (1999) Closed-Loop Identification Revisited. Journal of IFAC Automatica, 35, 1215-1241. DOI: 10.1016/S0005-1098(99)00022-9

Incropera, F. P., DeWitt, D. P., 2007. Fundamentals of Heat and Mass Transfer, 6th ed. John Wiley & Sons, Hoboken, NJ.

Ljung, L. 1999. System Identification: Theory for the User. Prentice Hall PTR, Linkoping University Sweden.

Moran, M. J., Shapiro, H. N., 2010. Fundamentals of Engineering Thermodynamics, 7th ed. John Wiley & Sons, Hoboken, NJ.

Pang, S., 2001. Improving MDF Fiber Drying Operation by Application of a Mathematical Model. Drying Technology, 19(8), 1789-1805. DOI: 10.1081/DRT-100107273

Rasekhi, S., Mazaeda, R., Tadeo, F., Garcia Bombin, A., 2025. Modelling a wood fiber flash dryer for MDF production. Jornadas de Automática, 46. DOI: 10.17979/ja-cea.2025.46.12115

Santos, P., Pitarch, J. L., de Prada, C., 2019. Energy-efficient operation of a medium-density fiberboard dryer through nonlinear MPC. IFAC-PapersOnLine, 52(1), 400-405. DOI: 10.1016/j.ifacol.2019.06.093

Santos, P., Pitarch, J. L., Vicente, A., de Prada, C., García, A., 2020. Improving operation in an industrial MDF flash dryer through physics-based NMPC. Control Engineering Practice, 94, 104213. DOI: 10.1016/j.conengprac.2019.104213